

Review Article

Continuous Backbone “Continuum” Robot Manipulators

Ian D. Walker

Department of Electrical and Computer Engineering, Clemson University, Clemson, SC 29634, USA

Correspondence should be addressed to Ian D. Walker; iwalker@clemson.edu

Received 8 May 2013; Accepted 4 June 2013

Academic Editors: J. Archibald and J. B. Koeneman

Copyright © 2013 Ian D. Walker. This is an open access article distributed under the Creative Commons Attribution License, which permits unrestricted use, distribution, and reproduction in any medium, provided the original work is properly cited.

This paper describes and discusses the history and state of the art of continuous backbone robot manipulators. Also known as continuum manipulators, these robots, which resemble biological trunks and tentacles, offer capabilities beyond the scope of traditional rigid-link manipulators. They are able to adapt their shape to navigate through complex environments and grasp a wide variety of payloads using their compliant backbones. In this paper, we review the current state of knowledge in the field, focusing particularly on kinematic and dynamic models for continuum robots. We discuss the relationships of these robots and their models to their counterparts in conventional rigid-link robots. Ongoing research and future developments in the field are discussed.

1. Introduction

Robotics as a field is still in its formative stages. Designers of robots are continuing to explore the range of possibilities for robot structures which can sense and perceive, navigate and locomote, as well as grasp and manipulate. The creation of programmable manipulators can be traced to be very beginning of robotics as a discipline [1]. To date, robot manipulators remain the core product of the field, being productively and profitably deployed in industrial settings worldwide.

However, when moving outside the highly structured world of industry, especially the factory floor, traditional rigid-link manipulators have been less successful. Their rigid-link structure (while excellent for precise positioning of their end effector) tends to be the cause of unwanted collisions when not in workcell environments specially engineered to maintain open spaces for their movements. Their inability to grasp objects other than at their end effector significantly restricts their manipulation capabilities beyond those of objects preengineered to fit their end effectors. Consequently, in real-world environments and situations not prechoreographed, it is generally nontrivial, and often not possible, to deploy rigid-link manipulators.

Robot manipulators do not, however, have to be formed from rigid-links. An alternative design possibility, which we

discuss in this paper, is to create a robot with a continuous form or backbone. These robots, termed *continuum robots*, can be viewed as being “invertebrate” robots, as compared with the “vertebrate” design of conventional rigid-link robots. Continuum robots can bend (and often extend/contract and sometimes twist) at any point along their structure. This provides them with capabilities beyond the scope of their rigid-link counterparts. An example (in the following paragraph) serves to illustrate this.

In Figure 1, a continuum robot gently contacts and adapts its shape to wrap around a fragile object (a glass lampshade). Subsequent to this image, the robot lifted and performed “whole arm manipulation” [2] of the object, without causing breakage or damage. This was achieved with no prior planning or knowledge of the object and without any sensing of the contact between robot and object. This would be an extremely difficult operation for a conventional rigid-link robot manipulator. Active force sensing would be required to present a sufficiently compliant interface to avoid breakage of the object. Further, note that even grasping such an object would require significant a priori specialized tooling or fixturing, as the object geometry is inherently unsuitable for grasping with a parallel jaw gripper. However, the continuum robot was able to use its compliant, actively controlled continuous structure to perform the operation easily, quickly, and without a priori knowledge or task engineering.



FIGURE 1: A continuum robot grasping and manipulating a fragile (glass) object, using its compliant backbone to adapt to the object's shape.

The above example of compliant whole arm grasping demonstrates one novel and appealing feature offered by continuum robots, compared to conventional rigid-link robots. Another key feature (and dual to the previous one above) is the potential to use the backbone to keep away from, rather than contract and grasp, complex environmental geometries. In this way, continuum backbones (note that the term backbone is used for continuum robots despite their invertebrate nature) can “twist and turn” to negotiate very tight spaces, thus penetrating areas where conventional robots would be unable to enter or would get their links stuck in. This novel potential and the attempt to realize that potential in useful hardware remain at the core of the field of continuum robots.

Historically, interest in continuous backbone robots began as early as the 1960s. As for the first continuum robot, Anderson and Horn’s Tensor Arm [3] (discussed further in Section 2) appears to have been the first prototype reported in the literature. Intended for underwater applications, the prototype did not, however, progress from the laboratory stage. It was quickly realized that, while early prototypes could be made to achieve a wide range of shapes, the relationship between the shapes and inputs was highly complex—much more than for rigid-link robots and certainly challenging for implementations using the computing environments of the time.

There followed a lull in activities in the area until the late 1980s and early 1990s, when two key developments occurred. Inspired by the need to approximate hyperredundant (rigid-link) robot backbones, Chirikjian published the first works [4, 5] providing general continuous backbone kinematics and dynamics for robots. Inspired by the example of snake locomotion, Hirose [6] published innovative results on the evolution of continuous backbone shapes. (Hirose also produced continuum robot prototypes [6]). Together, the above efforts are the seminal work establishing the field.

Further efforts in continuous backbone robot hardware in the 1990s centered in two directions: (1) extension of the original tendon-driven design concepts of Anderson/Horn and Hirose aimed at practical implementation [7, 8] and applications [9–11] and (2) the new innovation of creating backbones with pneumatically actuated chambers [12–14]. Robinson and Davies, codevelopers of some of the second

group of contributions, coined the term “continuum robot” in 1999 [15].

In parallel with the above developments in hardware, the 1990s saw progress and innovation in continuum robot modeling, particularly in kinematics. In a series of papers [16–18], “bottom-up” continuum robot kinematics models were developed. These works began with the constraints of physical continuum robot backbones and formulated backbone kinematics from them. It can be seen (this is reviewed in detail in Section 3) that the models resulting from these “bottom-up” approaches can be formed from the initially published “top-down” theory of [4, 5]. The new models, being matched directly to hardware constraints, enabled model-based implementations and thus real-time computer control of continuum robot shapes.

The late 1990s and the 2000s have seen a significant increase in the number of researchers in continuum robots and a corresponding increase in the number and breadth of published papers on the topic. In this paper, we review and discuss the current state of the art in the field of continuum robots. Summaries of early developments in the field have appeared [19, 20]. In this paper, we summarize the early work and update for the many recent developments in this rapidly emerging field. We begin in Section 2 by discussing the underlying design principles of continuum robots and classify continuum robot designs to date into three main design types. Section 3 provides an overview of the kinematics of continuum robots. The dynamics and control of continuum robots are reviewed and discussed in Section 4. Ongoing research in the field is summarized in Section 5. Conclusions follow in Section 6.

2. Design Principles

The defining feature of a continuum robot is a continuously curving core structure, or backbone, whose shape can be actuated in some way. An almost universal additional property is that the backbone is compliant; that is, it yields smoothly to externally applied loads. Together, these properties enable the physical capabilities which motivate continuum robots: to adapt the backbone shape to maneuver the robot within more complex environments and to conform to grasp a wider class of objects than feasible with rigid-link robots.

The design space available to achieve the above properties is very large. For example, the backbone core does not even have to be continuous. Snakes present the external appearance of having a continuous structure, but are vertebrates, with an internal segmented backbone comprised of (many very small) rigid-links. Robots with segmented rigid-link interior backbones presenting a continuous external form have been developed [8, 21–23]. These are sometimes termed “continuum-style” robots. However, such designs are rare, and almost all designers have sought to create truly continuous backbone structures. The most significant exceptions are the “snake-arms” [24] of OC Robotics [25], the only continuum-style robot currently commercially available. These robot arms, as the name suggests, are composed of

serially connected modular rigid-link sections. While not truly continuum, with enough modules, the form resembles a continuous backbone. They have been deployed in nuclear reactors and inside airframes, among other applications [25].

Design of robot structures in the absence of rigid elements is an unfamiliar process for most robotics designers. However, several fundamental design principles can be identified by a careful study of biological “tongues, trunks, and tentacles” [26–28]. In particular, the group of structures termed “muscular hydrostats” [29], which includes octopus arms, elephant trunks, squid tentacles, and mammalian tongues, has provided a rich vein of insight for continuum robot designers. Animals do not have to be the only source of inspiration; the vines and tendrils of plants [30] are a source of inspiration also [31, 32].

Muscular hydrostats are structures comprised almost entirely of their own actuators (muscle), with some additional fluid and connective tissue. They can typically bend and twist and often extend to some extent at any point along their structure. The muscles are arranged in oriented arrays (longitudinal, transverse, and oblique) in a way that enables both the motive force and structural support for bending, extension, and torsion to be provided by the muscles [29]. Some initial work [33] aimed to mimic (albeit at a much less detailed scale) the muscular hydrostat design concept in continuum robots, using various artificial muscle technologies. However, practical continuum robots require not only significant bending but also high force generation, and the state of the art in artificial muscle technology (both at the time of publication of [33] and at the time of writing this paper) was not capable of satisfying these needs at scales suitable for continuum robots. If, at some future time, artificial muscle technologies advance sufficiently, the possibilities for design and operation of continuum robots could be revolutionized [34]. Note that issues of packaging, power consumption, wiring, and so forth would remain major challenges.

In the absence of technologies which can easily mimic the key biological inspirations, designers have followed several alternative paths. The basic requirements are to produce active bending and ideally also some extension and local torsion, of continuous backbone structure which possesses some helpful (pre-designed) internal energy properties. Three alternative fundamental design strategies have emerged. Each strategy and notable continuum robots constructed to date using it are summarized in the following subsections.

2.1. Tendon-Based Designs. Perhaps the most direct approach to bending a continuous structure is the use of remotely actuated tendons. Given a backbone which, in the absence of external loads, consistently attains a given shape (typically a straight line, though this is not strictly necessary [35]), tendons can be used to deviate it from that shape via bending. Tendons are routed along the backbone and terminated in groups at selected points down it. Forces applied to the tendons at the base produce torques at the termination points, resulting in bending. The design is quite simple and (relatively) straightforward to realize in hardware.

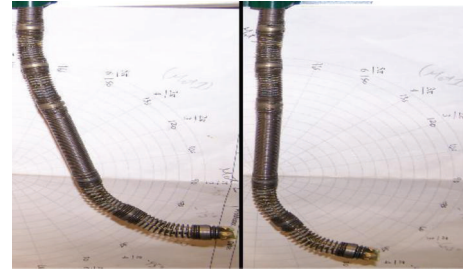


FIGURE 2: The Tendril, a tendon-driven continuum robot.

The first published example of a continuum robot, the “Tensor Arm” [3], is a good example of a tendon-based design. Tendons, routed through spacer elements, were used to effect bending of the core backbone element in several “sections.” The termination points of sets of tendons along the backbone define the sections; see Figure 2.

One choice for the core backbone element is a compressible spring. An early spring-backbone-based design was produced by Hirose [6]. The more recent long thin “Tendril” continuum robot by NASA Johnson Space Center [31] is also based on a spring backbone (Figure 2). The spring backbone provides natural compliance. However, this also makes the designs difficult to control, as control effort intended for backbone bending is lost in compression. The same is true for tendon-actuated pneumatic backbones (Figure 3).

A simple solution to the problem of uncontrolled compression is to use a flexible incompressible rod as the backbone element [7]; see Figure 4. This approach has several advantages including a slender low-profile backbone and more predictable behavior. The disadvantage of course is that this approach precludes the incorporation of backbone extension. However, the incompressible backbone concept has proved a popular and successful design, with numerous implementations based on it [36–39].

Tendon-based continuum designs share the following general features: (1) the backbone shape resolves into a finite series of “sections” whose end points are defined by the tendon termination points along the backbone; (2) the forces achievable with the device are relatively high (tendons generate relatively high forces); (3) some method must be found to prevent slack [17] and backlash [36] in the tendons; and (4) the design requires a relatively bulky actuator (motor) package at the base of the robot. With respect to (3), most implementations either actively actuate all tendons [40] or use a single actuator to actuate antagonistic tendon pairs, with a spring mechanism to take up the slack [17]. With respect to (4), the location of the actuator package outside the backbone has led to the tendon design being categorized as an “extrinsically actuated” continuum robot design [20].

Tendon-actuated continuum robots have been designed for space operations [31] and, in particular, medical procedures [40, 41]. A spring-based tendon-driven backbone continuum robot was developed for sinus surgery in [42] and another developed for ACL surgery in [43]. A system for laryngeal surgery was developed in [44]. A “robot octopus”



FIGURE 3: Air-Octor Continuum robot. This two-section, six-degree-of-freedom robot bends a pneumatically inflated core tube using six tendons.



FIGURE 4: Tendon-based continuum robot with incompressible flexible rod core.

with six cable-actuated limbs has been demonstrated underwater in [45].

2.2. Concentric Tube Designs. A second form of extrinsically actuated continuum robot (and the most recent to emerge) is based on a backbone formed by concentric compliant tubes. The tubes are free to move (translate and rotate) with respect to each other (subject to hardware limits) with the translations and rotations actuated at the base of the robot. The net effect is similar to some telescopes: the structure can extend and contract by translational sliding of the tubes longitudinally (modulo the length of the tubes, the smaller diameter tubes becoming the most distal), and the structure can achieve local rotation by rotational sliding of the tubes; see Figure 5.

The concentric tube design thus directly achieves both extension and torsion [46]. However, it does not inherently provide for backbone bending. The simplest approach to this issue is to use precurved compliant tubes [47, 48]. This, when combined with the directly controllable extension and torsion, provides some useful variation in backbone shapes. Another approach is to use tendons to bend the tubes [49, 50]. However, this significantly increases the complexity of the design [32].

Advantages of the concentric tube design include the inherently clean and thin design (assuming the design with no tendons to bend the tubes) and the fact that the actuator values (unlike with tendons) directly correspond to backbone

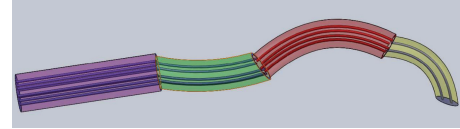


FIGURE 5: Concentric tube continuum robot concept.

shape variables. Disadvantages include the need for an external actuator package and the lack of inherent support for actively controlled bending.

Concentric tube continuum robots have found a niche application in the medical field, where their small profile and high compliance are well suited for minimally invasive procedures [49, 51, 52]. In this context, they are smaller-scale and lower-force devices than their counterparts constructed via the other two designs and are sometimes termed “active cannulas” [53]. For example, in [52], sampling-based motion planning techniques are used to design a concentric tube robot specifically for the task of navigation through the human lung. In [48], an MRI-compatible, piezoelectrically actuated concentric tube robot is designed for neurosurgery and percutaneous interventions.

2.3. Locally Actuated Backbone Designs. The third design type differs from the previous two by including the actuators directly in the backbone. Indeed, this type of “locally actuated” continuum robot typically forms the backbone from its actuators. In this regard, the design is closest to the biological continuum structures which often motivate continuum robots. This also gives rise to the categorization of the design as “intrinsically actuated” [20].

Typical locally actuated designs form the backbone from pneumatic “McKibben” muscles [54, 55], though numerous versions using shape memory alloys [56] have also been built. The strategy is to form the backbone from independently actuated sections. Each section is constructed from (typically) three independently actuated muscles, connected together along their length. The muscles can be “extenders” (increased length as a function of increased pressure) [54, 57] or “contractors” (decreased length as a function of higher pressure) [54, 58]. See Figure 6 for an example of the “Octarm” series of locally pneumatically actuated continuum robots.

When pressure is evenly increased or decreased in all three actuators of a straight section, the section length increases or decreases. When differing pressures are applied to the actuators, the section bends into a segment with approximately constant curvature. The plane of the curve is determined by the three pressures. In general, the section extends, contracts, and changes its curvature and plane of curvature as a function of the three applied pressures. The net shape of the backbone is thus a serially connected set of approximately constant curvature segments (with the end tangents coinciding).

The locally actuated continuum robot design has been the subject of much research and numerous realizations in the recent years. In particular, the high-profile “Octarm”

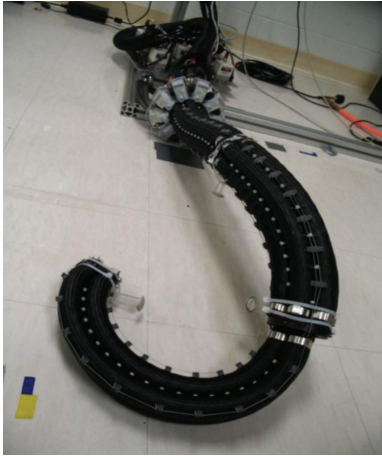


FIGURE 6: Intrinsically actuated three-section, nine-degree-of-freedom pneumatic “Octarm” continuum manipulator.

[33, 57, 59, 60] and “European Octopus” [45, 54, 61, 62] projects featured continuum robots based on this design. Other realizations of the design include the “Bionic Assistant” [35, 63], which closely resembles the trunk of an elephant [28]. Shape memory alloy actuation has been used to steer an active cannula for medical procedures, and in [64, 65], dual shape memory alloy-based backbones are used in a system designed for single port access surgery. Additionally, a locally actuated system for endoscopic stitching intended for surgical obesity treatment is presented in [66], and a design for colonoscopic insertion is described in [67].

Actuator selection for intrinsically actuated continuum robots can be from any available type of artificial muscle. This could include muscles based on engineered polymers, such as elastomers, for example. An extensive study of the potential of these types of actuators is presented in [34]. However, at this time, only the pneumatic or hydraulic actuator technologies feature the combination of bending and force generation capabilities for continuum robots at the human scale or larger.

Locally actuated continuum robot designs have the key advantage of inherently providing the backbone with extension, bending, and torsion (actually, bending in two dimensions). This is a feature not directly provided by either tendons or concentric tubes, as discussed in the preceding subsections. Disadvantages of locally actuated designs include relatively low force generation capabilities (for pneumatically actuated designs at least), fairly complex tube routing/valving, and the need for external pressure regulation equipment and a compressor.

2.4. Variable Backbone Stiffness. An interesting choice for continuum backbones is to use pneumatically actuated tubes. The KSI Tentacle Manipulator [11] and the Air-Octor robot ([68, 69] Figure 3) were each based on tendon-actuated extensible pneumatic chambers. This design allows tendon actuation of both bending and extension. Notice, however, that the pneumatically actuated tube design adds the

advantage of being able to actively regulate the internal stiffness of the backbone. However, these designs, in common with spring-based backbones, suffer from the problem of uncontrolled longitudinal compliance along the backbone. Also, pneumatics offer a limited range of possible backbone stiffnesses.

Alternative approaches to variable (controllable) stiffness backbones have considered magnetorheological and electrorheological fluid-based actuation [70, 71]. In these materials, magnetic and electric fields can be used to change the properties from fluid to stiff or solid. This allows backbones built from, or strongly biased by, such materials to feature tunable stiffness.

More recently, the idea of using “jamming” of suitable media (such as sand or coffee grains) has been exploited for novel variable stiffness continuum robot design [70, 72, 73]. The underlying notion is to pack the media in a closed chamber to bring and vary the internal pressure to “loosen” the media in a fluid state, or “jam” it into a solid state. For example, in [73], granular media are used as the jamming element. Initially packed into a chamber under a vacuum, the grains jam and unjam the chamber as a function of applied pressure. It is demonstrated in [73] that, when three such chambers are combined in parallel with a McKibben air muscle, a tunable stiffness section element can be produced. A prototype tendon-driven continuum robot using granular jamming for variable stiffness is demonstrated in [72].

In [70], the jamming elements are multiple surface layers, interleaved in various ways. Negative pressure is used to bring the layers together and exploit friction to create tunable stiffness via “layer jamming.” A tubular continuum backbone is built (locally actuated using shape memory alloy wires as core actuators) and shown to exhibit significant range of backbone stiffness. This approach to augmenting core continuum robot designs with new innovations to enhance performance shows significant promise for producing the next generation of continuum manipulators.

2.5. Common Property: Constant Curvature. Notice that, independent of underlying physical structure, a common property exhibited by virtually all continuum robots ([35, 63] being notable exceptions) is that the resulting backbone approximates a serially connected set of constant curvature sections. This arises due to the following: (1) all three previous design types create a series of serially connected sections; (2) internal potential energy in each section is uniformly distributed (unactuated, each section is straight, or bent at a fixed configuration); and thus, within each section, internal forces act to drive the unactuated (passive) degrees of freedom to equalize in value along the section. This produces internal section bending of constant curvature at any given moment.

Therefore, in practice, achievable continuum backbone shapes are (fairly close approximations to) sequentially connected segments of circles in three dimensions (with the tangents to successive section end points aligned and the arc lengths of the segments corresponding to robot section lengths). While the “constant curvature” property is affected

by external loading (some sag typically exists due to gravity or grasped objects), it remains a good first approximation to backbone shape and has been strongly exploited in kinematic models, as discussed in the next section.

3. Kinematics

In order to coordinate the movements available in continuum robots, kinematic models, which capture the relationship between configuration (backbone shape) variables and both task (e.g., tip) and actuator (e.g., tendon or muscle length), variables need to be established. Such models form the basis for motion planning and control algorithms and are the critical step between prototype development and practical implementation of continuum robot hardware.

Since continuum robots can change their shape at any point along their structure, their models necessarily differ significantly from those of conventional rigid-link robots, where configuration changes can occur only at a finite number of fixed locations along their structure (the joints between the rigid-links). For rigid-link robots, the well-established Denavit-Hartenberg (D-H) convention [1] provides a general underlying framework for the development of kinematic (and dynamic) models. The D-H convention establishes a local coordinate frame fixed in each of the (finite number of) links and develops the overall kinematics via a sequential series of frame-to-frame steps, as a function of the (finite) number of joint angles [1].

For continuum robots, the fact that the local shape varies continuously along the backbone needs to be reflected in kinematic models. Two alternative approaches have emerged. The first takes a “bottom-up” strategy, building a continuum model via exploiting the D-H approach to fit a “virtual” rigid-link robot to the backbone. The second uses a “top-down” philosophy, explicitly treating the backbone as a continuous curve, in order to formulate the models. We review each approach and demonstrate how ultimately they lead to the same models in the following two subsections.

3.1. Continuum Kinematics via Virtual Rigid-Link Kinematics. The first (and the most inspired by hardware) approach to continuum robot kinematics strongly exploits the constant curvature sections feature possessed by almost all continuum robots to date. This approach, which first appeared in [8], is based on the observation that the evolution from one end to the other of a constant curvature curve can be represented, in the plane of that curve, via three discrete transformations: (1) a rotation to “point” the tangent at the curve beginning to the curve end point; (2) a translation along the newly aligned direction (from curve beginning to end); and (3) a second rotation (of same amount as the first) to realign with the tangent at the curve’s end; see Figure 7.

Given this observation, in the plane, a “virtual” three-joint rigid-link manipulator, with identical (i.e., coupled) rotations as its first and third joints and a prismatic joint in the middle, can be used to model the kinematic transformation along any constant curvature backbone. Consequently, it is possible to find the corresponding kinematic model,

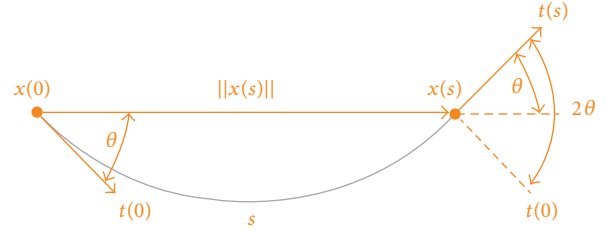


FIGURE 7: Geometry of constant curvature in the plane.

using the conventional D-H approach, for the virtual robot. This approach, first used in [8], has been used numerous times subsequently [18, 36, 39]. The details (D-H table and associated homogeneous transformation matrix) are given in Table 1 and (1).

Consider

$$[H_3^0] = \begin{bmatrix} \cos(\theta_1 + \theta_3) & -\sin(\theta_1 + \theta_3) & 0 & -d_2 \sin \theta_1 \\ \sin(\theta_1 + \theta_3) & \cos(\theta_1 + \theta_3) & 0 & d_2 \cos \theta_1 \\ 0 & 0 & 1 & 0 \\ 0 & 0 & 0 & 1 \end{bmatrix}. \quad (1)$$

Useful continuum robot kinematics can now be developed by noting, as well as substituting in the virtual robot kinematics, relationships between the joint variables for the virtual robot and corresponding configuration space variables for the continuous curve. Specifically (see Figure 7),

$$\theta_1 = \theta_3 = \theta, \quad d_2 = \|x(s)\|, \quad k = \left(\frac{1}{\text{radius}} \right). \quad (2)$$

We have (utilizing the underlying geometry)

$$s = r(2\theta) = \frac{(2\theta)}{k} = \frac{(\theta_1 + \theta_3)}{k}. \quad (3)$$

So

$$(\theta_1 + \theta_3) = sk. \quad (4)$$

Also

$$\frac{\|x(s)\|}{2} = \frac{d_2}{2} = r \sin \theta = \frac{\sin \theta}{k}. \quad (5)$$

So

$$d_2 = \frac{2 \sin \theta}{k}. \quad (6)$$

Substituting (4) and (6) into the model (1) and simplifying gives

$$[H_3^0] = \begin{bmatrix} \cos(sk) & -\sin(sk) & 0 & \left(\frac{1}{k}\right) \{\cos(sk) - 1\} \\ \sin(sk) & \cos(sk) & 0 & \left(\frac{1}{k}\right) \sin(sk) \\ 0 & 0 & 1 & 0 \\ 0 & 0 & 0 & 1 \end{bmatrix}. \quad (7)$$

TABLE 1

Link	θ	d	a	α
2	*	0	0	-90
3	0	*	0	90
3	*	0	0	0

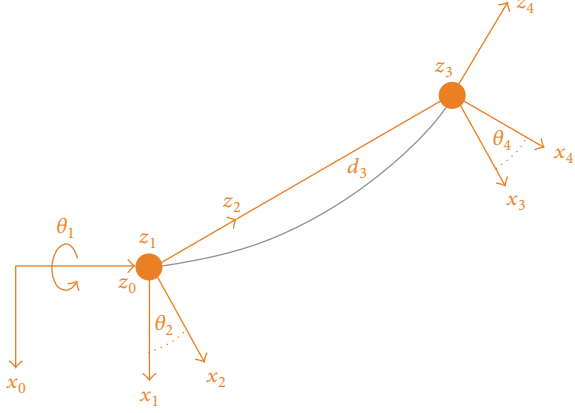


FIGURE 8: Three-dimensional constant curvature section geometry obtained via rotation about initial tangent.

The model (7) describes the forward kinematic relationship (3 by 3 orientation, top left of (7), and 3 by 1 translation, top right) between continuum curve shape (arc length and curvature) and task space. Note that the relationship is not, as for the rigid-link case, restricted to transformations from end to end of the “link” (“section” here). By making the arc length s arbitrary, the expression (7) models the transformation from curve shape to *any* task-space point along the backbone. Thus, the D-H algorithm for discrete jointed robots has been used to create a truly continuum section kinematic model in (7). Planar multisection kinematic models can be easily created by chaining together (multiplying the homogeneous transformation matrices) the models for the individual sections [17].

The kinematics of spatial constant curvature curves can similarly be modeled by the addition of an extra pair of (again identical, coupled) rotations to each end of the planar version to create a 3D virtual rigid-link robot. In a similar fashion, continuum kinematics are found by substitution of appropriate geometric relationships; see Figure 8 and Table 2. The 3D virtual robot is formally a 5-joint robot, with 2D rotational joints at each end of a prismatic joint. However, the robot has only three independent degrees of freedom, as the two 2D rotational joints are coupled. This agrees with the intuitive number of degrees of freedom of a constant curvature curve in space, that is, arc length, radius of curvature, and orientation of curve plane in space. Multisection 3D kinematic models can be created by chaining together individual section models as before [17].

3.2. “Direct” Continuum Kinematics Approach. An alternative (and more mathematically direct) approach explicitly treats the continuum backbone as a curve in space and “floats”

TABLE 2

Link	θ	d	a	α
1	*	0	0	90
2	*	0	0	-90
3	0	*	0	90
4	*	0	0	-90

a suitable coordinate system down the backbone. The position at σ along the backbone is found as (Φ is frame orientation)

$${}^0\mathbf{p}(\sigma, t) = \int_0^\sigma {}^0\Phi(\eta, t) \begin{bmatrix} 1 \\ 0 \\ 0 \end{bmatrix} d\eta. \quad (8)$$

The above equation reflects the model developed by Mochiyama and Suzuki [75–77], wherein the x -axis of the local coordinate system is aligned with the tangent down the backbone. An equivalent formulation developed earlier—the first kinematic analysis for continuum robot backbones—was developed by Chirikjian [4, 5]. In that formulation, the y -axis was aligned with the backbone tangent.

For the planar constant curvature section in Figure 7, the orientation matrix is given by

$${}^0\Phi(\sigma, t) = \begin{bmatrix} R_z^{\text{orientation}} \\ \cos\left(\int_0^\sigma k d\eta\right) & -\sin\left(\int_0^\sigma k d\eta\right) & 0 \\ \sin\left(\int_0^\sigma k d\eta\right) & \cos\left(\int_0^\sigma k d\eta\right) & 0 \\ 0 & 0 & 1 \end{bmatrix} \quad (9)$$

(k is the curvature). Utilizing (9) in (8) and performing the integration, we obtain

$${}^0\mathbf{p}(\sigma, t) = \begin{bmatrix} \left(\frac{1}{k}\right) \{\cos(k\sigma) - 1\} \\ \left(\frac{1}{k}\right) \sin(k\sigma) \\ 0 \end{bmatrix}. \quad (10)$$

Noting that

$${}^0\Phi(\sigma, t) = \begin{bmatrix} \cos\left(\int_0^\sigma k d\eta\right) & -\sin\left(\int_0^\sigma k d\eta\right) & 0 \\ \sin\left(\int_0^\sigma k d\eta\right) & \cos\left(\int_0^\sigma k d\eta\right) & 0 \\ 0 & 0 & 1 \end{bmatrix} \quad (11)$$

$$= \begin{bmatrix} \cos(k\sigma) & -\sin(k\sigma) & 0 \\ \sin(k\sigma) & \cos(k\sigma) & 0 \\ 0 & 0 & 1 \end{bmatrix},$$

and recalling that

$$[H_3^0] = \begin{bmatrix} {}^0\Phi(\sigma, t) & {}^0\mathbf{p}(\sigma, t) \\ 0 & 1 \end{bmatrix}^0. \quad (12)$$

We obtain (noting the “0” in the previous equation is a 1 by 3 vector)

$$[H_3^0] = \begin{bmatrix} \cos(sk) & -\sin(sk) & 0 & \left(\frac{1}{k}\right)\{\cos(sk) - 1\} \\ \sin(sk) & \cos(sk) & 0 & \left(\frac{1}{k}\right)\sin(sk) \\ 0 & 0 & 1 & 0 \\ 0 & 0 & 0 & 1 \end{bmatrix}. \quad (13)$$

Note that the resulting model in (13) is identical to the one obtained in (7). A similar parallel calculation can be performed to generate the 3D kinematic model. Note that the model suffers from singularities (division by zero) when the curvature is zero or when any section is straight.

Consequently, we have established a baseline kinematic model relating backbone shape to task-space variables, independent of the approach used to find it.

3.3. Modal Approaches. The previous approaches establish kinematics which directly model the nominal shapes the robots can obtain. However, they are fairly complex to formulate and manipulate. An alternative strategy is to “build” backbone shapes via a finite number of relatively simple modal functions. Originally introduced to robotics in [78] (in which the resulting shapes were used to plan movements for hyperredundant rigid-link robots), the modal approach builds the kinematics using as backbone curvature:

$$k(s) = \sum_{i=1}^n \mu_i \phi_i(s), \quad (14)$$

where μ_i are coefficients, and $\phi_i(s)$ are the modal functions. The modal functions act as “basis” functions for the backbone curvature, with the coefficients selected to tune their combination to approximate (or, in some special cases, match) the robot backbone shape [16, 78]. The coefficients become the “configuration” of the robot.

The (number and type of) modal functions can be selected from a wide range of possibilities [16, 78, 79]. For example, in [78], Chirikjian and Burdick used the following model:

$$k(s) = \sum_{i=1}^n \mu_i \cos(i\pi s) + \beta_i \sin(i\pi s). \quad (15)$$

In this model, the configuration becomes $q = [\mu_1(t), \beta_1(t), \dots, \beta_i(t)\mu_i(t), \dots, \mu_n(t), \beta_n(t)]$. The use of the classical trigonometric basis functions appears a natural choice. However, an infinite number of trigonometric modes are needed to model an arbitrary backbone shape. Also, this basis set provides no spatial resolution (each basis function affects the shape of the whole robot); so it is not possible to “tune” a given region of the backbone.

It is sometimes possible to select modal functions to achieve spatial resolution. In [16], (the first few elements of) two alternative sets of Wavelet basis functions are used. These

use the “natural basis set” or “box functions” (left column in Figure 9):

$$k(s) = \sum_{i=1}^n \mu_i \phi_i^b(s) \quad (16)$$

and the “Haar” basis set (right column in Figure 9):

$$k(s) = \sum_{i=1}^n \mu_i \phi_i^w(s). \quad (17)$$

The natural basis set comprises “box functions,” with (fixed) support, chosen to match the backbone region of (nonextensible, planar) sections, and with the box magnitudes corresponding directly to the curvature of those sections. The effect of using this basis set is illustrated in Figure 9 (column 2) to successively (top to bottom) form a specific shape for a four-section planar backbone. Note that the natural basis set features fixed spatial resolution at variable locations along the backbone.

The (first four elements of the) Haar basis set (both sets are orthogonal sets in the sense of Wavelet bases) is shown in the right hand column, top to bottom, of Figure 9. These functions feature variable spatial resolution, at variable locations. However, for this particular example, it can be seen that they can also be combined (top to bottom, third column of Figure 9) to produce the same shape as with the natural basis set.

Note that the natural basis “box” functions in Figure 9 directly synthesize the kinematics for four constant curvature sections. This is an example of exact modal function modeling. However, the box function approach is not generalized to extensible sections or to 3D backbones; so this is a (convenient) special case.

The key advantage of the modal function approach is that the robot shape can be parameterized by a finite set of user-selected functions with convenient properties. The number of “modes” used can be user-selected, for example, to constrain the computational complexity of the resulting model. Modal models can be synthesized to eliminate the singularities inherent in the models of Sections 3.1 and 3.2 (when sections straighten and curvature is zero) [79].

The main disadvantage of modal function-based approaches is that they are inherently approximations: most modal function sets which are convenient to manipulate require many (typically, infinite) numbers of them to achieve a given backbone shape. Most importantly, the set of shapes available in the model is inherently restricted by the range of (linear combinations of) the modal basis functions. For many modal function sets, even if an infinite number is used, it is not possible to model an arbitrary backbone shape. Therefore, some physically achievable backbone shapes may not be included in the modal models. This particularly is a problem for 3D backbones [16]. Therefore, the use of modal function approaches typically needs to be augmented with additional analysis of and compensation for the inherent mismatch between models and hardware.

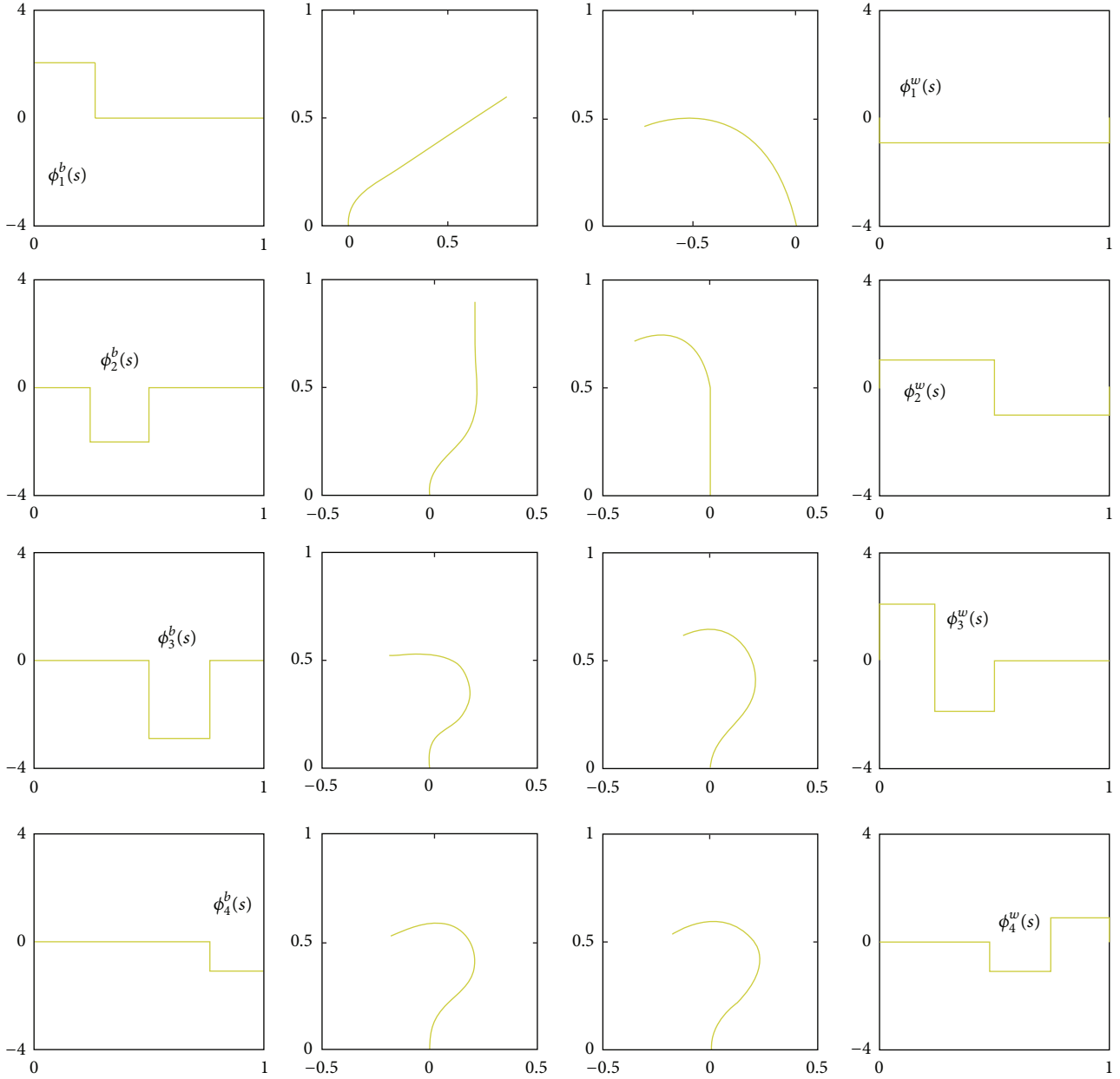


FIGURE 9: Construction of four-section planar continuum backbone shape via alternative modal basis sets. Left column: first four elements (top to bottom) of natural basis set. Right column: first four elements (top to bottom) of Haar basis set. Second column: backbone shape generation (top to bottom), adding successive natural basis functions. Third column: backbone shape generation (top to bottom), adding successive Haar basis functions.

3.4. Kinematic Transformations Incorporating Actuator Variables. Kinematic backbone models are very useful and provide key insight into the possible configurations and behavior of continuum robots. However, for practical implementation of continuum robot realizations, even at the kinematic level, further modeling is required. In the case of rigid-link robots, the variables underlying their kinematic models (joint angles and displacements) correspond closely to actuator geometry. Conversion between configuration and actuator variables (typically involving gear/belt/drive reduction ratios) is relatively straightforward [1]. However, for continuum

robots, the relationship between the key variables defining backbone configuration (extension, curvature, and torsion) and actuated variables is considerably more complex.

For example, consider tendon-based continuum robots. Here, the only actuated (and, often, sensed) variables are tendon lengths, and it is desirable in practice to be able to convert these tendon lengths to backbone configuration (extension, curvature, torsion). This issue has been addressed in [18], and in the following, we summarize the solution for the case of a single (extensible) section with circular cross-section, actuated by three tendons, spaced at 120 degrees

apart around the section perimeter. A good example of such a section is the “Air-Octor” continuum robot [68, 69], illustrated in Figure 10.

For the continuum section in Figure 10 (the kinematics are similar, if not identical, for the sections of almost all tendon-driven continuum robots), the forward problem is to find the section shape from the three tendon lengths l_{1-3} . The shape is given by the three configuration space variables: section length s , curvature k_ϕ , and angle of curvature (from the x -axis, measured about the z -axis of a coordinate frame with its z -axis aligned with the base tangent of the section) (see Figure 11).

The key to developing the needed transformations is to exploit the geometric constraints of the design. The three tendons are routed through a series of $n - 1$ intermediate connection points before being terminated at the end of the section. During actuation, this causes the tendons to form n straight line segments within the section. Straightforward geometrical analysis can be used to show that the length h_c of a (imaginary) tendon running directly through the center of a single such segment of the section is given by

$$h_c = \frac{l_3 + l_2 - 2l_1}{6n}, \quad (18)$$

where the shortest tendon length is l_1 , and n is the number of segments in the section. This length can be used to analyze the “side-on” geometry (Figure 12).

Use of the geometric information in Figure 12 and a projection onto the (z, ϕ) plane results [18] in expressions for the curvature and angle of curvature in terms of tendon lengths

$$k_\phi = 2 \frac{\sqrt{l_1^2 + l_2^2 + l_3^2 - l_1 l_2 - l_2 l_3 - l_1 l_3}}{d(l_1 + l_2 + l_3)}, \quad (19)$$

$$\phi = \tan^{-1} \left(\frac{\sqrt{3} l_3 + l_2 - 2l_1}{3(l_2 - l_3)} \right),$$

where d is the radius of the section cross-section, and r_1 is the inverse of its curvature. Finally, after some further geometrical analysis, it can be shown that [18]:

$$s = \frac{nd(l_1 + l_2 + l_3)}{\sqrt{l_1^2 + l_2^2 + l_3^2 - l_1 l_2 - l_2 l_3 - l_1 l_3}} \cdot \sin^{-1} \left(\frac{\sqrt{l_1^2 + l_2^2 + l_3^2 - l_1 l_2 - l_2 l_3 - l_1 l_3}}{3nd} \right). \quad (20)$$

Equations (19) and (20) constitute the needed forward map between actuator and shape variables for tendon-driven extensible sections. Further work on kinematic transformations can be found in [18, 80, 81]. For example, in [80], a mechanics-based model for transforming between beam configuration and tendon displacements is formulated. Inverse maps can also be formulated [81, 82]. It is fairly straightforward to chain together multiple section models to model a multisection robot; see [18] for details.

The aforementioned models are critical in implementation of tendon-based continuum robots. They can be easily modified for locally actuated designs, where tendon lengths are replaced by internal actuator lengths. Finally, note that the concentric tube realization of continuum robots presents a distinct advantage in the context of kinematic transformations, as the local extension and torsion (of each tube section) are directly actuated, and thus no kinematic transformation between these configuration and actuation variables is required.

3.5. Extensions, Inverse and Velocity Kinematics. The kinematics formulations in Sections 3.1–3.4 represent the core theory underlying continuum robots and have been the subject of much of the theoretical research activity in the area thus far. Extensions to this core theory have been developed and there remains active research in the area. In particular, efforts to remove the restriction to constant curvature sections have been made.

More accurate kinematic models which explicitly include the effects of external (particularly gravitational) loading have been explored in the literature. The theory of Cosserat Rods has proved particularly helpful in enabling researchers to develop “geometrically exact” nonconstant curvature kinematic models [37, 60, 83]. However, the models are computationally complex [60] and harder to implement than the constant curvature models. Consequently, the constant curvature models remain predominant in continuum robot implementations.

Inverse models (including those for both the configuration-workspace transformations of Sections 3.1–3.3 and the actuator-configuration relationships of Section 3.4) have been developed in [74] (for nonconstant curvature models), [79, 82].

Various approaches to exploiting the kinematic relationships to formulate and exploit Jacobians which reflect the velocity-level kinematic relationships have been proposed [16, 74, 84]. Conventional techniques for formulating Jacobians for rigid-link robots can be applied to the “virtual” rigid-link manipulator of Section 3.1 to derive a “continuum” Jacobian. More directly, any of the kinematic relationships (modal or direct) can be differentiated to find the appropriate Jacobian. A Jacobian (pseudo-) inverse can then be used to iteratively solve configuration space rates given desired tip rates. For example, the modal function approach for the planar four-degree-of-freedom example in Section 3.3 can be used to derive

$$\frac{d\underline{x}(s)}{dt} = [J(\underline{\mu}, s)] \frac{d\underline{\mu}}{dt}, \quad (21)$$

thus formulating the Jacobian and its relationship in terms of the modal function coefficients and their time derivatives [16]. Inverting this relationship yields model coefficient (and hence shape) rates which can be numerically integrated to provide shape trajectories corresponding to the input tip rates. See Figure 13 for an example trajectory generated for the example robot of Section 3.3 using this approach.

Research into continuum robot kinematics continues. For example, an alternative (screw theoretic) approach to

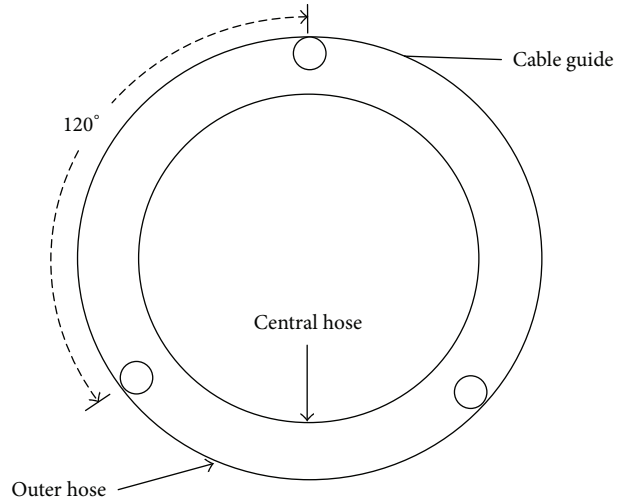
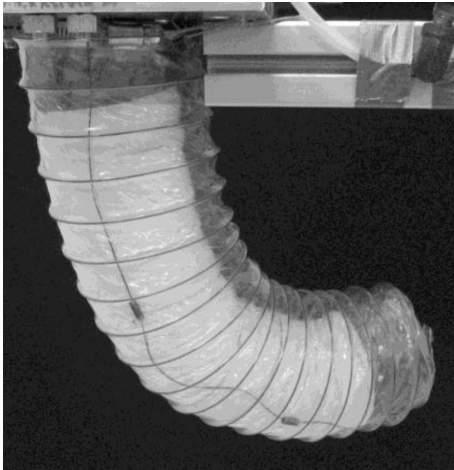


FIGURE 10: The single-section “Air-Octor.” Internal hose is pressurized; external hose is actuated (two independent degrees of freedom bending, plus one of extension) by three remotely actuated tendons, terminated at the end of the section and spaced 120 degrees apart around its perimeter.

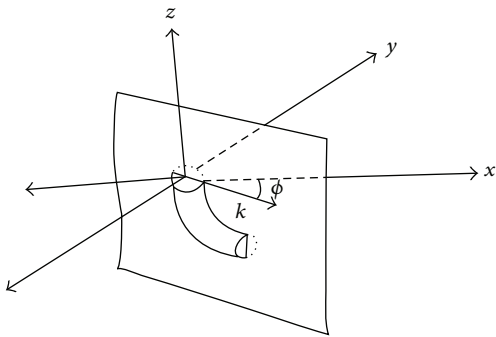


FIGURE 11: Definition of section configuration space variables for curvature and angle of curvature.

the development of both kinematics and Jacobian formulation, using the “product of exponentials” approach, is given recently in [39]. The approach is shown to produce the same results as using the models described previously.

4. Forces, Dynamics, and Control

4.1. Forces and Continuum Robots. The natural next step in modeling of continuum robots is to include the relationships involving forces (and moments) and backbone shape and shape changes. For conventional rigid-link robots, the kinematic variables (joint angles/displacements) completely determine the shape (configuration) of the robot. However, for continuum robots, external forces (in particular, gravity) act with the configuration variables and the internal energy of the backbone to determine the ultimate shape of each section [19, 47], even in free space. In any physically realizable system, there can be only a finite number of actuated (i.e., directly controlled) configuration degrees of freedom. The values of the remainder of the (infinite) degrees of freedom in

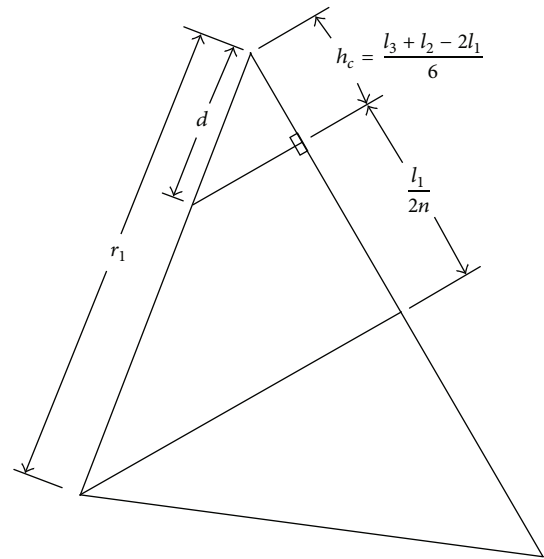


FIGURE 12: View from side of one segment of section.

a continuum robot backbone will be determined by both the constraints of the controlled degrees of freedom and internal and external forces.

The kinematic models of Section 3 made no explicit assumptions of internal or external loading. Implicitly, the constant curvature assumptions in Section 3 assumed no external loading and an even distribution of internal loading within each section (to even out the uncontrolled degrees of freedom to create the constant curvature). In practice, gravitational loads cause some “section sag,” resulting in section curvatures that are not truly constant. However, the deviation from constant curvature in free space is typically not large, and the constant curvature models have proved

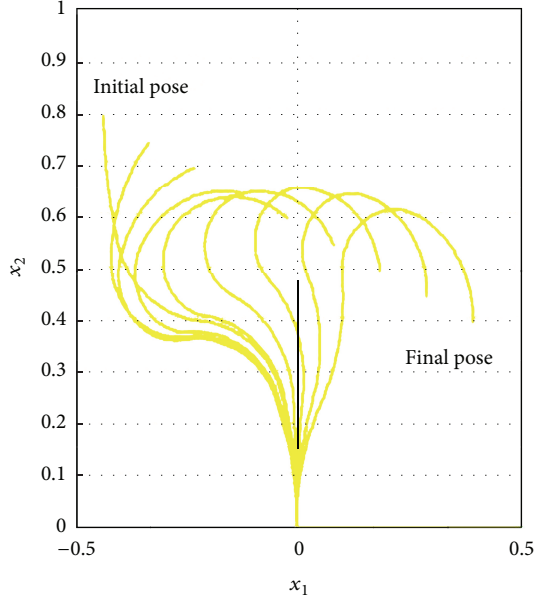


FIGURE 13: Straight line tip trajectory for four-section planar continuum robot, generated using Jacobian from modal kinematics.

a good practical approximation in many implementations [17, 59, 63].

However, as applications become more challenging, the desire for more accurate models is increasing. Internal loads can play a significant role in determining the shape of concentric tube robots in particular. In [47], a quasistatic model for predicting the shape of concentric tube robots is presented. The model in [47] takes internal forces from both bending and shear effects into account. Mechanics-based models which consider torsional interaction between the tubes of concentric tube robots are presented in [85]. Lumped-parameter models to model friction within a continuum catheter device are presented in [86].

More accurate kinematic models which explicitly include the effects of external (particularly, gravitational) loading have been explored in the literature [37, 83]. However, these models are relatively complex. Consequently, the constant curvature models remain predominant in continuum robot implementations.

External loading becomes a much more significant factor when the loads result from environmental contact, however. In this case (inevitable when using continuum elements for locomotion and actively sought when using them for grasping and manipulation), the inherent compliance of the continuum structures allows for significant deviation from constant curvature. Notice that this deviation is inevitable—the finite number of actuated degrees of freedom cannot, in general, be made to control the infinite number of other degrees of freedom in the structure, in the presence of general and significant external forces. The deviation is also a desired property, in order to allow the robot to adapt its shape to environmental constraints, both for navigation and grasping.

In order to address some of these issues, new work considers applied loading. A solution to the statics problem

for concentric tube robots is presented in [87]. An approach to continuum backbone contact detection and location of contact along the backbone is developed in [88]. Methods based on kinematics and statics are presented, supported by experimental results with a tendon-driven continuum backbone. Recent extensions [38] present algorithms (supported by experimental results) to register and locate continuum backbones under external contact conditions with respect to an a priori 3D model.

A novel alternative strategy is to explicitly use continuum robots as force sensors [37]. In [37], an Extended Kalman Filter approach is used with a tendon-driven continuum robot to provide tip force estimates given kinematic models and estimates.

4.2. Continuum Robot Dynamics. The earliest published work on continuum robot dynamics, based on a modal model, was [5]. Subsequent efforts based on the well-understood [1] Lagrangian [75, 76, 89, 90] and Newton-Euler [61, 91, 92] methods have been established. In the following, we outline the Lagrangian dynamics approaches [75, 76, 90], which generally parallel the commonly used formulation for rigid-link robots. However, there are several steps which are both specialized to continuum robot scenario and which give good insight into the nature of continuum robots.

The key initial step [75] is to model the backbone as being comprised of circular cross-sectional “slices,” of infinitesimal thickness. Each slice, at a location σ along the backbone, has mass $m(\sigma)$, inertia tensor $I(\sigma)$, and first moment of inertia $m(\sigma)r(\sigma)$, where $r(\sigma)$ is the distance from the slice geometric center to its center of mass. The overall strategy is to find the kinetic and potential energy of each slice, then the total energies K and P (via integration along the backbone), and finally substitute $L = K - P$ into Lagrange’s equations ($i = 1, \dots, n$)

$$\frac{d}{dt} \left[\frac{\partial L}{\partial \dot{\theta}_i(\sigma, t)} \right] - \frac{\partial L}{\partial \theta_i(\sigma, t)} = \tau_i(\sigma, t) \quad (22)$$

to find the dynamic model. In the above, (θ_i, τ_i) are variables selected to correspond to the n actuated configuration space variables and the corresponding forces which change them.

The kinetic energy of a slice (assuming the center of mass is aligned with the geometric center of the slice) is most directly given by

$$\begin{aligned} K(\sigma, t) &= \left(\frac{1}{2} \right) m(\sigma) \left\{ \frac{\partial \mathbf{p}(\sigma, t)}{\partial t} \right\}^T \left\{ \frac{\partial \mathbf{p}(\sigma, t)}{\partial t} \right\} \\ &+ \left(\frac{1}{2} \right) \boldsymbol{\omega}(\sigma, t)^T I(\sigma) \boldsymbol{\omega}(\sigma, t) \\ &\triangleq \left(\frac{1}{2} \right) \nu(\sigma, t)^T M(\sigma, t) \nu(\sigma, t), \end{aligned} \quad (23)$$

where $\{\partial \mathbf{p}(\sigma, t)/\partial t, \boldsymbol{\omega}(\sigma, t)\}$ are the linear and angular velocities of the slice center at σ .

An additional step (analogous to the process for rigid-link robot Lagrangian dynamics) is now necessary. In order to obtain the dynamics in terms of the useful variables (θ_i, τ_i) ,

a (Jacobian) transformation must be found to convert $v(\sigma, t)$ in the above to $\partial\theta(\sigma, t)/\partial t$. This Jacobian needs to account for the phenomenon that the velocity at σ is a function of the velocities at all locations η prior to it along the backbone. To this end, intermediate Jacobians $[J_1]$, $[J_2]$ are found such that

$$\begin{aligned} \begin{bmatrix} \mathbf{v}(\sigma) \\ \boldsymbol{\omega}(\sigma) \end{bmatrix} &= [J_1] \begin{bmatrix} \mathbf{v}(\eta) \\ \boldsymbol{\omega}(\eta) \end{bmatrix}, \\ \begin{bmatrix} \mathbf{v}(\eta) \\ \boldsymbol{\omega}(\eta) \end{bmatrix} &= [J_2] \frac{\partial\theta(\eta, t)}{\partial t}, \end{aligned} \quad (24)$$

and a desired overall Jacobian operator $[J_{(\sigma,t)}]$ is found as

$$v(\sigma, t) = [J_{(\sigma,t)}] \left\{ \frac{\partial\theta}{\partial t} \right\} = \int_0^\sigma [J_1] [J_2] \frac{\partial\theta(\eta, t)}{\partial t} d\eta. \quad (25)$$

For full details, see [75].

Thus, the kinetic energy of a slice can now be represented as

$$K(\sigma, t) = \left(\frac{1}{2} \right) \left\{ \frac{\partial\theta}{\partial t} \right\}^T J_{(\sigma,t)}^T M(\sigma) J_{(\sigma,t)} \left\{ \frac{\partial\theta}{\partial t} \right\}. \quad (26)$$

The overall kinetic energy is therefore

$$K(t) = \int_0^l K(\sigma, t) d\sigma, \quad (27)$$

where l is the length of the backbone. The potential energy of a slice is found as

$$P_g(\sigma, t) = -m(\sigma) \mathbf{g}^T(\sigma, t) \mathbf{p}(\sigma, t), \quad (28)$$

where \mathbf{g} is the gravitation vector at σ . The overall potential energy given by

$$P_g(t) = \int_0^l P_g(\sigma, t) d\sigma = - \int_0^l m(\sigma) \mathbf{g}^T(\sigma, t) \mathbf{p}(\sigma, t) d\sigma. \quad (29)$$

After forming $L = K - P$ and substituting into Lagrange's equations (22), the resulting dynamic model takes the form

$$\mathbf{M}\ddot{\mathbf{q}} + \mathbf{V}(\mathbf{q}, \dot{\mathbf{q}}) \dot{\mathbf{q}} + \mathbf{g}(\mathbf{q}) = \boldsymbol{\tau}. \quad (30)$$

The underlying structure of the dynamic model closely matches that of rigid-link robots, apart from being continuous in nature. For example, the inertia matrix M can be shown [90, 93] to be positive definite and symmetric, and it satisfies the property (useful for control)

$$\xi^T (\dot{M} - 2V) \xi = 0, \quad \forall \xi \in \mathbb{R}^n. \quad (31)$$

The original derivation of (30) [75] assumed fixed length (i.e., nonextensible) backbones and the only potential energy in the system arose from gravity. Later work [90] generalized the models to include extensible sections, and the effects of elastic internal potential energy due to both bending and extension. The corresponding energy terms are

$$P_b(t) = \left(\frac{1}{2} \right) \int_0^l k_b(\sigma) \left\{ \pi - \left(\frac{1}{2} \right) \sigma \kappa(\sigma) \right\}^2 d\sigma \quad (32)$$

for bending (spring constant k_b) and

$$P_e(t) = \left(\frac{1}{2} \right) k_e (l - l^*)^2 \quad (33)$$

for extension (spring constant k_e). Details of application of the previous approach to compute the dynamics for extensible and nonextensible backbones are given in [90].

Establishing the previous closed form dynamic models for continuum robots has been significant in yielding insight into the underlying structure of these devices. The structure of the model is useful in synthesizing control strategies [93, 94], and the dynamics enables realistic physics-based simulations of continuum robots. However, the computational complexity of the resulting model is very high, and the calculations for nonplanar backbones are nontrivial. Real-time implementation of these models (even with the simplifying assumptions of simple mass distribution) is a daunting prospect.

Consequently, researchers have explored alternative approaches to dynamic modeling for continuum robots. Formulations based on the iterative Newton-Euler approach have been established [61, 91, 92]. More recently, computationally (more) efficient lumped-parameter models, based on linear mass-spring-damper elements, have appeared in the literature [95–97]. The model in [97] is tuned to octopus-inspired underwater operation and includes terms to model buoyancy and drag. These approaches approximate the dynamics of (sections of) continuum backbones by various combinations of linear elements, with a view of trading off computational complexity of the model against accuracy. Experiments have shown good correspondence between the models and hardware, for relatively a small number (less than twenty) of linear elements [95].

Dynamic models for nonconstant curvature continuum robots are beginning to appear in the literature [83]. However, at the time of this writing, there are very few examples of continuum dynamics being implemented on continuum robot hardware. It is expected that, as applications expand, particularly in areas such as medical procedures and locomotion with continuum limbs, the availability of dynamics in real time will become increasingly necessary. Research in continuum robot dynamics continues to be a very active area.

4.3. Continuum Robot Control. Controller development for robotic structures is a fundamental issue, and several of the early works [98, 99] in continuum robots concentrated on this topic. Control of continuum structures is obviously complicated by the inherently underactuated nature of the backbone. Additional problems arise from the (typical) non-collocation of actuators with configuration space variables, the complexity of the dynamic models, and the typical dearth of local sensors in the structure.

For tendon-based continuum robots particularly, the existence of kinematic transformations between configuration space and actuator space variables is critical in enabling effective control. Controllers specific to tendon-based continuum robots have been presented in [80, 81, 83]. Stiffness

controllers for continuum robots are introduced in [46]. In [46], a Cosserat Rod model is used to calculate the tip deflection due to applied forces, enabling implementation of stiffness control. The approach is applied in [46] to a concentric tube robot, but the modeling strategy (combining noncontact kinematics as in Section 3 with the Cosserat Rod model to include applied forces) is applicable to other continuum robot designs as well.

Control strategies attempting to compensate for the complexity of the dynamics or for the uncertainty inherently present in implementation of dynamic models are presented in [98–100]. Inverse dynamics controllers are described in [100]. In [99, 100], variable structure controllers are proposed. A feedforward neural network approach for compensation for the dynamics is discussed in [94]. Controllers in the task space are presented in [49, 100]. A controller based on a mechanics model describing coupling between sections is presented in [81].

A key practical problem for continuum robot control is at which level to close the loop. Sensors are typically noncollocated with the backbone. Sensed quantities are usually limited to tendon lengths (sensed at the base), or pneumatic or hydraulic pressures of artificial muscles (again, sensed remotely at pressure regulators, not at the muscles themselves). Direct internal sensing of backbone shape is complicated by the limited space available and the current lack of suitable sensor technologies. Technologies based on fiber optics offer promise for low-profile, high-quality local sensing of backbone curvature. However, this has not yet been demonstrated in continuum robot hardware. Consequently, transformations between actuator and configuration space become important for controller implementation, with the loop closed (error calculated) in either space.

External sensing of continuum robot shape has also been demonstrated. Electromagnetic field sensors were used in [36] to sense the shape of tendon-driven endoscopic systems. Vision has been used to infer the shape of continuum robots in [101] (off-board cameras) and [102] (body-mounted cameras), but the effectiveness of this strategy is limited by issues of lighting conditions, occlusions, and so forth. Vision has also been used to sense backbone tip location [81]. An electromagnetic sensor is used in [49] to sense tip location and enable task-space control.

5. Ongoing Research

With the field rapidly expanding and the core underlying theory having been established over the last ten to fifteen years, a wider variety of issues and problems are now being considered by researchers. New work in motion planning for continuum robots [52, 85, 103–105] is expanding the boundaries of the possible for the field. Motion planners based on mechanics models for concentric tube robots are presented in [85, 103]. Planners have been proposed which use the structure of continuum backbones to plan trajectories which simultaneously avoid obstacles and grasp objects. These planners are proposed for both 2D [105] and 3D [103]

environments and are intended for real-time, or near real-time, implementation [103]. Extensions for moving obstacles can be handled [105]. The emergence of low-cost and readily available sensors such as the Kinect RGB-D sensor catalyzes this type of research.

The existence of practical, real-time, sensor-based motion planning algorithms will be important in moving the technology from the laboratory to numerous real applications [106]. Currently, most of the higher-level functions (including planning) are delegated to humans. Most implementations to this point require teleoperation of the device [107], typically using a joystick [108]. User interfaces for continuum robots is a relatively neglected and poorly understood topic [108]. The movements of continuum elements are often counterintuitive to human operators, much more than for rigid-link robots, leading to confusion and slow or poor decision making in many experiments. Efforts to reduce operator cognitive load via automatic motion planning and the synthesis of low degree of freedom “synergies” [109, 110] are expected to prove significant in widening the scope and effectiveness of possible operations.

Recent theoretical work has investigated the structure of the “self-motion” inherent in continuum structures [111]. This self-motion (movement of the backbone while maintaining the location of the tip), present in kinematically redundant robots, has proved useful in conventional rigid-link manipulators. Multisection continuum robots are inherently kinematically redundant, but, apart from its proposed use in task-space control strategies [100], their self-motion remains a little studied phenomenon.

The use of continuum robot structures as limbs for “legged” locomotion has recently been the subject of attention [61, 112, 113]. Demonstration of multicontinuum-limbed locomotion has been reported both underwater [33, 45], and in air [112]. Multi- (two-) continuum-limbed swimming is analyzed with feasibility demonstrated via a simple prototype in [114]. Multicontinuum-legged robots have been demonstrated to walk and trot [112]. Possible applications for this novel locomotion mode include various undersea and space applications. Other space-based applications in which continuum robots could be used effectively are as “active hooks” [113] and as long, thin “tendrillike” robots [31, 115–117]. In the latter mode, the robots could penetrate and explore within tight obstacle fields such as crevasses, lava tubes, or skylights, where key scientific questions are currently focused.

Novel applications are emerging. Continuum robots have been deployed recently as “active hoses” for ship-to-shore refueling [118]. Extension to continuum robot surfaces, with application to rehabilitation therapy for poststroke patients, has been proposed [119].

6. Conclusions

We have reviewed the state of the art in continuum manipulators, focusing particularly on hardware design, kinematics, and dynamics. The design of continuum robot hardware is seen to have evolved into three fundamentally different

directions. Two of these directions feature out-of-backbone “extrinsic” actuation: one via remote actuation via tendons and the other via remotely actuated sliding of concentric tubes. The third direction forms the continuum backbone from the actuators themselves and is hence termed “intrinsically actuated.” Actuator selection for intrinsically actuated continuum robots can be from any available type of artificial muscle. This could include pneumatic “McKibben” muscles, hydraulically actuated muscles, muscles based on novel polymers, or shape memory alloys, for example. However, at this time only the pneumatic or hydraulic actuator technologies feature the combination of bending and force generation capabilities for continuum robots at the human scale or larger. At a large scale, the extrinsic tendon-driven designs have the advantage of high force capability. At the small scale, the concentric tendon design has advantages and is already showing promise in numerous medical applications.

Understanding of the kinematics of continuum robots has been the subject of much research and has now reached a mature stage, with theory matching most of the corresponding results for rigid-link robots now established. Indeed, key aspects of the core theory for rigid-link robots can be used to form a baseline model for continuum robot kinematics, as has been discussed herein. Alternatively, the same models can be derived from first principles, and the results are seen to be equivalent. However, continuum robot kinematics modeling presents issues and difficulties not present for rigid-link robots, due to the inherent compliance and infinite degrees of freedom present in continuum robot backbones. Models which take into account the effects on the kinematics from external loading such as from gravity have been established. However, the additional computational complexity in these models remains to be a barrier to implementation at this time.

Computational complexity is also a significant issue in the study and application of continuum robot dynamics, and related subfields. As discussed herein, traditional methods for dynamics formulation, such as the Lagrangian and Newton-Euler approaches, can be extended and adapted to form continuum robot dynamic models. These models are seen to possess the same key structural properties as for rigid-link robots, encouraging the development of corresponding control strategies. However, the continuous nature of the continuum backbone renders these models extremely computationally complex. Some recent work has developed less computationally complex approximate dynamic models. However, at this time, few dynamics-based implementations have been reported, and continuum robot dynamics and control remain active research issues.

Taking advantage of the previous developments, research into continuum robots is actively expanding at the time of writing this paper. New work in areas such as motion planning and contact modeling is extending our underlying body of understanding and widening the scope of the field. Researchers are partnering with various industries to explore continuum robot solutions to such diverse applications such as terrain-adapting continuum-limbed vehicles, ship-to-ship refueling, and exploration of extraterrestrial surfaces. It is

anticipated that the next ten years will see an explosion of research, both basic and applied, in the area of continuum robots.

Acknowledgments

This research was supported in part by NASA under NRI Contract NNX12AM01G and in part by the U.S. National Science Foundation under Grant IIS-0904116.

References

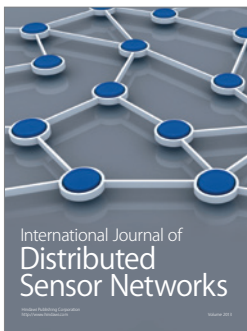
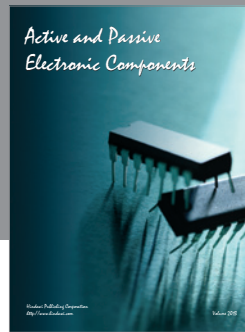
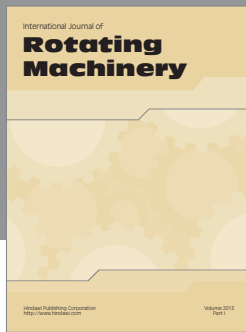
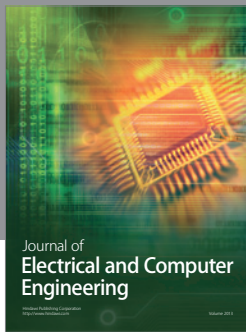
- [1] M. W. Spong, S. Hutchinson, and M. Vidyasagar, *Robot Modeling and Control*, Wiley, 2006.
- [2] J. K. Salisbury, “Whole arm manipulation,” in *Proceedings of the 4th Symposium on Robotics Research*, MIT Press, 1987.
- [3] V. C. Anderson and R. C. Horn, “Tensor arm manipulator design,” *Transactions of the ASME*, vol. 67, DE-57, pp. 1–12, 1967.
- [4] G. S. Chirikjian, *Theory and applications of hyperredundant robotic mechanisms [Ph.D. thesis]*, Department of Applied Mechanics, California Institute of Technology, 1992.
- [5] G. S. Chirikjian, “Hyper-redundant manipulator dynamics: a continuum approximation,” *Advanced Robotics*, vol. 9, no. 3, pp. 217–243, 1994.
- [6] S. Hirose, *Biologically Inspired Robots*, Oxford University Press, 1993.
- [7] I. A. Gravagne, C. D. Rahn, and I. D. Walker, “Large deflection dynamics and control for planar continuum robots,” *IEEE/ASME Transactions on Mechatronics*, vol. 8, no. 2, pp. 299–307, 2003.
- [8] M. W. Hannan and I. D. Walker, “Analysis and experiments with an elephant’s trunk robot,” *Advanced Robotics*, vol. 15, no. 8, pp. 847–858, 2001.
- [9] R. Cieślak and A. Morecki, “Elephant trunk type elastic manipulator—a tool for bulk and liquid materials transportation,” *Robotica*, vol. 17, no. 1, pp. 11–16, 1999.
- [10] G. Immega, “Tentacle-like Manipulators with adjustable tension lines,” U.S. Patent 5317952, 1992.
- [11] G. Immega and K. Antonelli, “KSI tentacle manipulator,” in *Proceedings of the 1995 IEEE International Conference on Robotics and Automation. Part 1 (of 3)*, pp. 3149–3154, Nagoya, Japan, May 1995.
- [12] D. M. Lane, J. B. C. Davies, G. Robinson et al., “The AMADEUS dextrous subsea hand: design, modeling, and sensor processing,” *IEEE Journal of Oceanic Engineering*, vol. 24, no. 1, pp. 96–111, 1999.
- [13] K. Suzumori, S. Iikura, and H. Tanaka, “Development of flexible microactuator and its applications to robotic mechanisms,” in *Proceedings of the IEEE International Conference on Robotics and Automation*, pp. 1622–1627, April 1991.
- [14] J. F. Wilson, D. Li, Z. Chen, and R. T. George, “flexible robot manipulators and grippers: relatives of elephant trunks and squid tentacles,” in *Robots and Biological Systems: Towards a New Bionics?* vol. 102, pp. 474–479, 1993.
- [15] G. Robinson and J. B. C. Davies, “Continuum robots—a state of the art,” in *Proceedings of the IEEE International Conference on Robotics and Automation (ICRA ’99)*, pp. 2849–2854, May 1999.
- [16] I. Gravagne and I. D. Walker, “Kinematics for constrained continuum robots using wavelet decomposition,” in *Proceedings of the 4th International Conference and Exposition/Demonstration*

- on *Robotics for Challenging Situations and Environments*, pp. 292–298, Albuquerque, NM, USA, March 2000.
- [17] M. W. Hannan and I. D. Walker, “Kinematics and the implementation of an elephant’s trunk manipulator and other continuum style robots,” *Journal of Robotic Systems*, vol. 20, no. 2, pp. 45–63, 2003.
- [18] B. A. Jones and I. D. Walker, “Kinematics for multisection continuum robots,” *IEEE Transactions on Robotics*, vol. 22, no. 1, pp. 43–55, 2006.
- [19] D. Trivedi, C. D. Rahn, W. M. Kier, and I. D. Walker, “Soft robotics: biological inspiration, state of the art, and future research,” *Applied Bionics and Biomechanics*, vol. 5, no. 3, pp. 99–117, 2008.
- [20] R. J. Webster III and B. A. Jones, “Design and kinematic modeling of constant curvature continuum robots: a review,” *International Journal of Robotics Research*, vol. 29, no. 13, pp. 1661–1683, 2010.
- [21] T. Aoki, A. Ochiai, and S. Hirose, “Study on slime robot development of the mobile robot prototype model using bridle bellows,” in *Proceedings of the IEEE International Conference on Robotics and Automation*, pp. 2808–2813, New Orleans, La, USA, May 2004.
- [22] H. Ohno and S. Hirose, “Design of slim slime robot and its gait of locomotion,” in *Proceedings of the IEEE/RSJ International Conference on Intelligent Robots and Systems*, pp. 707–715, Maui, Hawaii, USA, November 2001.
- [23] H. Tsukagoshi, A. Kitagawa, and M. Segawa, “Active hose: an artificial elephant’s nose with maneuverability for rescue operation,” in *Proceedings of the IEEE International Conference on Robotics and Automation*, pp. 2454–2459, Seoul, Korea, May 2001.
- [24] R. Buckingham, “Snake arm robots,” *Industrial Robot*, vol. 29, no. 3, pp. 242–245, 2002.
- [25] R. Buckingham, OC Robotics, <http://www.ocrobotics.com/>.
- [26] F. W. Grasso, “Octopus sucker-arm coordination in grasping and manipulation,” *American Malacological Bulletin*, vol. 24, no. 1-2, pp. 13–23, 2008.
- [27] J. L. Van Leeuwen and W. M. Kier, “Functional design of tentacles in squid: linking sarcomere ultrastructure to gross morphological dynamics,” *Philosophical Transactions of the Royal Society B*, vol. 352, no. 1353, pp. 551–571, 1997.
- [28] F. Martin and C. Niemitz, “How do African elephants (*Loxodonta africana*) optimize goal-directed trunk movements?” in *Jahresversammlung der Dt. Zool. Ges. und der Dt. Ges. f. Parasitologie*, vol. 96, Berlin, Germany, 2003.
- [29] W. M. Kier and K. K. Smith, “Tongues, tentacles and trunks: the biomechanics of movement in muscular-hydrostats,” *Zoological Journal of the Linnean Society*, vol. 83, no. 4, pp. 307–324, 1985.
- [30] A. Goriely and S. Neukirch, “Mechanics of climbing and attachment in twining plants,” *Physical Review Letters*, vol. 97, no. 18, Article ID 184302, 2006.
- [31] J. S. Mehling, M. A. Diftler, M. Chu, and M. Valvo, “A minimally invasive tendril robot for in-space inspection,” in *Proceedings of the 1st IEEE/RAS-EMBS International Conference on Biomedical Robotics and Biomechatronics (BioRob ’06)*, pp. 690–695, February 2006.
- [32] I. D. Walker, “Robot strings: long, thin continuum robots,” in *Proceedings of the IEEE Aerospace Conference*, pp. 1–12, Big Sky, Mont, USA, 2013.
- [33] I. D. Walker, D. M. Dawson, T. Flash et al., “Continuum robot arms inspired by cephalopods,” in *Unmanned Ground Vehicle Technology VII*, Proceedings of SPIE, pp. 303–314, Orlando, Fla, USA, March 2005.
- [34] J. Bishop-Moser, G. Krishnan, C. Kim, and S. Kota, “Design of soft robotic actuators using fluid-filler fiber-reinforced elastomeric enclosures in parallel combinations,” in *Proceedings of the IEEE/RSJ International Conference on Intelligent Robot Systems (IROS ’12)*, pp. 4262–4269, Vilamoura, Portugal, 2012.
- [35] A. Grzesiak, R. Becker, and A. Verl, “The bionic handling assistant: a success story of additive manufacturing,” *Assembly Automation*, vol. 31, no. 4, pp. 329–333, 2011.
- [36] B. Bardou, P. Zanne, F. Nageotte, and M. De Mathelin, “Control of a multiple sections flexible endoscopic system,” in *Proceedings of the 23rd IEEE/RSJ 2010 International Conference on Intelligent Robots and Systems (IROS ’10)*, pp. 2345–2350, Taipei, Taiwan, October 2010.
- [37] D. C. Rucker and R. J. Webster III, “Deflection-based force sensing for continuum robots: a probabilistic approach,” in *Proceedings of the IEEE/RSJ International Conference on Intelligent Robots and Systems: Celebrating 50 Years of Robotics (IROS ’11)*, pp. 3764–3769, San Francisco, Calif, USA, September 2011.
- [38] S. Tully, A. Bajo, G. Kantor, H. Choset, and N. Simaan, “Constrained filtering with contact detection for the localization and registration of continuum robots in flexible environments,” in *Proceedings of the IEEE International Conference on Robotics and Automation*, pp. 3388–3394, St. Paul, Minn, USA, 2012.
- [39] Q. Zhao and F. Gao, “Design and analysis of a kind of biomimetic continuum robot,” in *Proceedings of the IEEE International Conference on Robotics and Biomimetics (ROBIO ’10)*, pp. 1316–1320, Tianjin, China, December 2010.
- [40] J. Shang, C. J. Payne, J. Clark et al., “Design of a multitasking robotic platform with flexible arms and articulated hand for minimally invasive surgery,” in *Proceedings IEEE/RSJ International Conference on Intelligent Robot Systems (IROS ’12)*, pp. 1998–1993, Vilamoura, Portugal, 2012.
- [41] G. Chen, P. M. Tu, T. R. Herve, and C. Prelle, “Design and modeling of a micro-robotic manipulator for colonoscopy,” in *Proceedings of the 5th International Workshop on Research and Education in Mechatronics*, pp. 109–114, Annecy, France, 2005.
- [42] H.-S. Yoon, S. M. Oh, J. H. Jeong et al., “Active bending endoscope robot system for navigation through sinus area,” in *Proceedings of the IEEE/RSJ International Conference on Intelligent Robots and Systems: Celebrating 50 Years of Robotics (IROS ’11)*, pp. 967–972, San Francisco, Calif, USA, September 2011.
- [43] H. Watanabe, K. Kanou, Y. Kobayashi, and M. G. Fujie, “Development of a “steerable drill” for ACL reconstruction to create the arbitrary trajectory of a bone tunnel,” in *Proceedings of the IEEE/RSJ International Conference on Intelligent Robots and Systems: Celebrating 50 Years of Robotics (IROS ’11)*, pp. 955–960, San Francisco, Calif, USA, September 2011.
- [44] N. Simaan, R. Taylor, and P. Flint, “A dexterous system for laryngeal surgery,” in *Proceedings of the IEEE International Conference on Robotics and Automation*, pp. 351–357, New Orleans, La, USA, May 2004.
- [45] M. Calisti, A. Arienti, F. Renda et al., “Design and development of a soft robot with crawling and grasping capabilities,” in *Proceedings of the IEEE International Conference on Robotics and Automation*, pp. 4950–4955, St. Paul, Minn, USA, 2012.
- [46] M. Mahvash and P. E. Dupont, “Stiffness control of a continuum manipulator in contact with a soft environment,” in *Proceedings of the 23rd IEEE/RSJ 2010 International Conference on Intelligent*

- Robots and Systems (IROS '10)*, pp. 863–870, Taipei, Taiwan, October 2010.
- [47] J. Lock, G. Laing, M. Mahvash, and P. E. Dupont, “Quasistatic modeling of concentric tube robots with external loads,” in *Proceedings of the 23rd IEEE/RSJ 2010 International Conference on Intelligent Robots and Systems (IROS '10)*, pp. 2325–2332, Taipei, Taiwan, October 2010.
- [48] H. Su, D. C. Cardona, W. Shang et al., “A MRI-guided concentric tube continuum robot with piezoelectric actuation: a feasibility study,” in *Proceedings IEEE International Conference on Robotics and Automation*, pp. 1939–1945, St. Paul, Minn, USA, 2012.
- [49] R. S. Penning, J. Jung, N. J. Ferrier, and M. R. Zinn, “An evaluation of closed-loop control options for continuum manipulators,” in *Proceedings of the IEEE International Conference on Robotics and Automation*, pp. 5392–5397, St. Paul, Minn, USA, 2012.
- [50] A. Degani, H. Choset, A. Wolf, T. Ota, and M. A. Zenati, “Percutaneous intrapericardial interventions using a highly articulated robotic probe,” in *Proceedings of the 1st IEEE/RAS-EMBS International Conference on Biomedical Robotics and Biomechatronics (BioRob '06)*, pp. 7–12, Pisa, Italy, February 2006.
- [51] E. J. Butler, R. Hammond-Oakley, S. Chawarski et al., “Robotic neuro-endoscope with concentric tube augmentation,” in *Proceedings of the IEEE/RSJ International Conference on Intelligent Robot Systems (IROS '12)*, pp. 2941–2946, Vilamoura, Portugal, 2012.
- [52] L. G. Torres, R. J. Webster III, and R. Alterovitz, “Task-oriented design of concentric tube robots using mechanics-based models,” in *Proceedings of the IEEE/RSJ International Conference on Intelligent Robots and Systems (IROS '12)*, pp. 4449–4455, Vilamoura, Portugal, 2012.
- [53] R. J. Webster III, J. M. Romano, and N. J. Cowan, “Kinematics and calibration of active cannulas,” in *Proceedings of the IEEE International Conference on Robotics and Automation (ICRA '08)*, pp. 3888–3895, Pasadena, Calif, USA, May 2008.
- [54] E. Guglielmino, N. Tsagarakis, and D. G. Caldwell, “An octopus anatomy-inspired robotic arm,” in *Proceedings of the 23rd IEEE/RSJ 2010 International Conference on Intelligent Robots and Systems (IROS '10)*, pp. 3091–3096, Taipei, Taiwan, October 2010.
- [55] M. B. Pritts and C. D. Rahn, “Design of an artificial muscle continuum robot,” in *Proceedings of the IEEE International Conference on Robotics and Automation*, pp. 4742–4746, New Orleans, La, USA, May 2004.
- [56] E. Ayvali and J. P. Desai, “Towards a discretely actuated steerable cannula,” in *Proceedings of the IEEE International Conference on Robotics and Automation*, pp. 1614–1619, St. Paul, Minn, USA, 2012.
- [57] B. A. Jones, M. Csencsits, W. McMahan et al., “Grasping, manipulation, and exploration tasks with the OctArm continuum manipulator,” in *Proceedings of the International Conference on Robotics and Automation*, Orlando, Fla, USA, 2006.
- [58] A. Bartow, A. Kapadia, and I. D. Walker, “A novel continuum trunk robot based on contractor muscles,” in *Proceedings of the 12th WSEAS International Conference on Signal Processing, Robotics, and Automation*, pp. 181–186, Cambridge, UK, 2013.
- [59] W. McMahan, V. Chitrakaran, M. Csencsits et al., “Field trials and testing of “OCTARM” continuum robots,” in *Proceedings of the IEEE International Conference on Robotics and Automation (ICRA '06)*, pp. 2336–2341, May 2006.
- [60] D. Trivedi, A. Lotfi, and C. D. Rahn, “Geometrically exact dynamic models for soft robotic manipulators,” in *Proceedings of the IEEE/RSJ International Conference on Intelligent Robots and Systems (IROS '07)*, pp. 1497–1502, San Diego, Calif, USA, November 2007.
- [61] R. Kang, E. Guglielmino, D. T. Branson, and D. G. Caldwell, “Bio-Inspired crawling locomotion of a multi-arm octopus-like continuum system,” in *Proceedings of the IEEE/RSJ International Conference on Intelligent Robots and Systems (IROS '12)*, pp. 145–150, Vilamoura, Portugal, 2012.
- [62] C. Laschi, B. Mazzolai, V. Mattoli, M. Cianchetti, and P. Dario, “Design of a biomimetic robotic octopus arm,” *Bioinspiration and Biomimetics*, vol. 4, no. 1, Article ID 015006, 2009.
- [63] M. Rolf and J. J. Steil, “Constant curvature continuum kinematics as fast approximate model for the bionic handling assistant,” in *Proceedings of the IEEE/RSJ International Conference on Intelligent Robot Systems (IROS '12)*, pp. 3440–3446, Vilamoura, Portugal, 2012.
- [64] J. Ding, K. Xu, R. E. Goldman, P. K. Allen, D. L. Fowler, and N. Simaan, “Design, simulation and evaluation of kinematic alternatives for insertable robotic effectors platforms in single port access surgery,” in *Proceedings of the IEEE International Conference on Robotics and Automation (ICRA '10)*, pp. 1053–1058, Anchorage, Alaska, USA, May 2010.
- [65] K. Xu, R. E. Goldman, J. Ding, P. K. Allen, D. L. Fowler, and N. Simaan, “System design of an insertable robotic effector platform for Single Port Access (SPA) surgery,” in *Proceedings of the IEEE/RSJ International Conference on Intelligent Robots and Systems (IROS '09)*, pp. 5546–5552, St. Louis, MO, USA, October 2009.
- [66] K. Xu, J. Zhao, J. Geiger, A. J. Shih, and M. Zheng, “Design of an endoscopic stitching device for surgical obesity treatment using a N.O.T.E.S approach,” in *Proceedings of the IEEE/RSJ International Conference on Intelligent Robots and Systems: Celebrating 50 Years of Robotics (IROS '11)*, pp. 961–966, San Francisco, Calif, USA, September 2011.
- [67] S. Wakimoto and K. Suzumori, “Fabrication and basic experiments of pneumatic multi-chamber rubber tube actuator for assisting colonoscope insertion,” in *Proceedings of the IEEE International Conference on Robotics and Automation (ICRA '10)*, pp. 3260–3265, Anchorage, Alaska, USA, May 2010.
- [68] B. A. Jones, W. McMahan, and I. D. Walker, “Design and analysis of a novel pneumatic manipulator,” in *Proceedings of the 3rd IFAC Symposium on Mechatronic Systems*, pp. 745–750, Sydney, Australia, 2004.
- [69] W. McMahan, B. A. Jones, and I. D. Walker, “Design and implementation of a multi-section continuum robot: air-octor,” in *Proceedings of the IEEE IRS/RSJ International Conference on Intelligent Robots and Systems (IROS '05)*, pp. 3345–3352, Edmonton, Canada, August 2005.
- [70] Y. J. Kim, S. Cheng, S. Kim, and K. Iagnemma, “Design of a tubular snake-like manipulator with stiffening capability by layer jamming,” in *Proceedings of the IEEE/RSJ International Conference on Intelligent Robot Systems (IROS '12)*, pp. 4251–4256, Vilamoura, Portugal, 2012.
- [71] A. Sadeghi, L. Beccai, and B. Mazzolai, “Innovative soft robots based on electro-rheological fluids,” in *Proceedings of the IEEE/RSJ International Conference on Intelligent Robot Systems (IROS '12)*, pp. 4237–4242, Vilamoura, Portugal, 2012.
- [72] N. G. Cheng, M. B. Lobovsky, S. J. Keating et al., “Design and analysis of a robust, low-cost, highly articulated manipulator enabled by jamming of granular media,” in *Proceedings of the*

- IEEE International Conference on Robotics and Automation*, pp. 4328–4333, St. Paul, Minn, USA, 2012.
- [73] A. Jiang, G. Xynogalas, P. Dasgupta, K. Althoefer, and T. Nanayakkara, “Design of a variable stiffness flexible manipulator with composite granular jamming and membrane coupling,” in *Proceedings IEEE/RSJ International Conference on Intelligent Robots and Systems (IROS '12)*, pp. 2922–2927, Vilamoura, Portugal, 2012.
- [74] M. Giorelli, F. Renda, M. Calisti, A. Arienti, G. Ferri, and C. Laschi, “A two dimensional inverse kinetics model of a cable-driven manipulator inspired by the octopus arm,” in *Proceedings of the IEEE International Conference on Robotics and Automation*, pp. 3819–3824, St. Paul, Minn, USA, 2012.
- [75] H. Mochiyama and T. Suzuki, “Dynamics modeling of a hyperflexible manipulator,” in *Proceedings of the 41st SICE Annual Conference*, pp. 1505–1510, Osaka, Japan, 2002.
- [76] H. Mochiyama and T. Suzuki, “Kinematics and dynamics of a cable-like hyper-flexible manipulator,” in *Proceedings of the IEEE International Conference on Robotics and Automation*, pp. 3672–3677, Taipei, Taiwan, September 2003.
- [77] H. Mochiyama, “Whole-arm impedance of a serial-chain manipulator,” in *Proceedings of the IEEE International Conference on Robotics and Automation*, pp. 2223–2228, Seoul, Korea, May 2001.
- [78] G. S. Chirikjian and J. W. Burdick, “Modal approach to hyper-redundant manipulator kinematics,” *IEEE Transactions on Robotics and Automation*, vol. 10, no. 3, pp. 343–354, 1994.
- [79] I. S. Godage, E. Guglielmino, D. T. Branson, G. A. Medrano-Cerda, and D. G. Caldwell, “Novel modal approach for kinematics of multisection continuum arms,” in *Proceedings of the IEEE/RSJ International Conference on Intelligent Robots and Systems: Celebrating 50 Years of Robotics (IROS '11)*, pp. 1093–1098, San Francisco, Calif, USA, September 2011.
- [80] D. B. Camarillo, C. F. Milne, C. R. Carlson, M. R. Zinn, and J. K. Salisbury, “Mechanics modeling of tendon-driven continuum manipulators,” *IEEE Transactions on Robotics*, vol. 24, no. 6, pp. 1262–1273, 2008.
- [81] D. B. Camarillo, C. R. Carlson, and J. K. Salisbury, “Task-space control of continuum manipulators with coupled tendon drive,” in *Experimental Robotics: The 11th International Symposium*, O. Khatib, V. Kumar, and G. Pappas, Eds., pp. 271–280, Springer, 2009.
- [82] S. Neppalli, M. A. Csencsits, B. A. Jones, and I. D. Walker, “Closed-form inverse kinematics for continuum manipulators,” *Advanced Robotics*, vol. 23, no. 15, pp. 2077–2091, 2009.
- [83] F. Renda and C. Laschi, “A general mechanical model for tendon-driven continuum manipulators,” in *Proceedings of the IEEE International Conference on Robotics and Automation*, pp. 3813–3818, St. Paul, Minn, USA, 2012.
- [84] I. A. Gravagne and I. D. Walker, “Manipulability, force, and compliance analysis for planar continuum manipulators,” *IEEE Transactions on Robotics and Automation*, vol. 18, no. 3, pp. 263–273, 2002.
- [85] L. G. Torres and R. Alterovitz, “Motion planning for concentric tube robots using mechanics-based models,” in *Proceedings of the IEEE/RSJ International Conference on Intelligent Robots and Systems: Celebrating 50 Years of Robotics (IROS '11)*, pp. 5153–5159, San Francisco, Calif, USA, September 2011.
- [86] J. Jung, R. S. Penning, N. J. Ferrier, and M. R. Zinn, “A modeling approach for continuum robotic manipulators: effects of nonlinear internal device friction,” in *Proceedings of the IEEE/RSJ International Conference on Intelligent Robots and Systems: Celebrating 50 Years of Robotics (IROS '11)*, pp. 5139–5146, San Francisco, Calif, USA, September 2011.
- [87] D. C. Rucker, B. A. Jones, and R. J. Webster III, “A model for concentric tube continuum robots under applied wrenches,” in *Proceedings of the IEEE International Conference on Robotics and Automation (ICRA '10)*, pp. 1047–1052, Anchorage, Alaska, USA, May 2010.
- [88] A. Bajo and N. Simaan, “Finding lost wrenches: using continuum robots for contact detection and estimation of contact location,” in *Proceedings of the IEEE International Conference on Robotics and Automation (ICRA '10)*, pp. 3666–3673, Anchorage, Alaska, USA, May 2010.
- [89] I. S. Godage, D. T. Branson, E. Guglielmino, G. A. Medrano-Cerda, and D. G. Caldwell, “Shape function-based kinematics and dynamics for variable-length continuum robotic arms,” in *Proceedings of the IEEE International Conference on Robotics and Automation*, pp. 452–457, Shanghai, China, September 2011.
- [90] E. Tatlicioglu, I. D. Walker, and D. M. Dawson, “New dynamic models for planar extensible continuum robot manipulators,” in *Proceedings of the IEEE/RSJ International Conference on Intelligent Robots and Systems (IROS '07)*, pp. 1485–1490, San Diego, Calif, USA, November 2007.
- [91] R. Kang, A. Kazakidi, E. Guglielmino et al., “Dynamic model of a hyper-redundant, octopus-like manipulator for underwater applications,” in *Proceedings of the IEEE/RSJ International Conference on Intelligent Robots and Systems: Celebrating 50 Years of Robotics (IROS '11)*, pp. 4054–4059, San Francisco, Calif, USA, September 2011.
- [92] W. Khalil, G. Gallot, O. Ibrahim, and F. Boyer, “Dynamic modeling of a 3-D serial eel-like robot,” in *Proceedings of the IEEE International Conference on Robotics and Automation*, pp. 1270–1275, Barcelona, Spain, April 2005.
- [93] A. Kapadia, E. Tatlicioglu, D. Dawson, and I. D. Walker, “A new approach to extensible continuum robot control using the sliding-mode,” *Computer Technology and Application*, vol. 2, no. 4, pp. 293–300, 2011.
- [94] D. Braganza, D. M. Dawson, I. D. Walker, and N. Nath, “Neural network grasping controller for continuum robots,” in *Proceedings of the 45th IEEE Conference on Decision and Control (CDC '06)*, pp. 6445–6449, San Diego, Calif, USA, December 2006.
- [95] N. Giri and I. D. Walker, “Three module lumped element model of a continuum arm section,” in *Proceedings of the IEEE/RSJ International Conference on Intelligent Robots and Systems: Celebrating 50 Years of Robotics (IROS '11)*, pp. 4060–4065, San Francisco, Calif, USA, September 2011.
- [96] R. S. Penning, J. Jung, J. A. Borgstadt, N. J. Ferrier, and M. R. Zinn, “Towards closed loop control of a continuum robotic manipulator for medical applications,” in *Proceedings IEEE International Conference on Robotics and Automation*, pp. 4822–4827, 2011.
- [97] T. Zheng, D. T. Branson III, R. Kang et al., “Dynamic continuum arm model for use with underwater robotic manipulators inspired by *Octopus vulgaris*,” in *Proceedings of the IEEE International Conference on Robotics and Automation*, pp. 5289–5294, St. Paul, Minn, USA, 2012.
- [98] M. Ivanescu, N. Bizdoaca, and D. Pana, “Dynamic control for a tentacle manipulator with SMA actuators,” in *Proceedings of the IEEE International Conference on Robotics and Automation*, pp. 2079–2084, Taipei, Taiwan, September 2003.

- [99] M. Ivanescu and V. Stoian, "A Variable structure controller for a tentacle manipulator," in *Proceedings of the 1995 IEEE International Conference on Robotics and Automation. Part 1 (of 3)*, pp. 3155–3160, May 1995.
- [100] A. Kapadia and I. D. Walker, "Task-space control of extensible continuum manipulators," in *Proceedings of the IEEE/RSJ International Conference on Intelligent Robots and Systems: Celebrating 50 Years of Robotics (IROS '11)*, pp. 1087–1092, San Francisco, Calif, USA, September 2011.
- [101] M. W. Hannan and I. D. Walker, "Real-time shape estimation for continuum robots using vision," *Robotica*, vol. 23, no. 5, pp. 645–651, 2005.
- [102] B. Weber, P. Zeller, and K. Kuhnlenz, "Multi-camera based real-time configuration estimation of continuum robots," in *Proceedings IEEE/RSJ International Conference on Intelligent Robot Systems (IROS '12)*, pp. 3550–3555, Vilamoura, Portugal, 2012.
- [103] J. Li and J. Xiao, "Determining "grasping" configurations for a spatial continuum manipulator," in *Proceedings of the IEEE/RSJ International Conference on Intelligent Robots and Systems: Celebrating 50 Years of Robotics (IROS '11)*, pp. 4207–4214, San Francisco, Calif, USA, September 2011.
- [104] L. A. Lyons, R. J. Webster III, and R. Alterovitz, "Planning active cannula configurations through tubular anatomy," in *Proceedings of the IEEE International Conference on Robotics and Automation (ICRA '10)*, pp. 2082–2087, Anchorage, Alaska, USA, May 2010.
- [105] J. Xiao and R. Vatcha, "Real-time adaptive motion planning for a continuum manipulator," in *Proceedings of the 23rd IEEE/RSJ 2010 International Conference on Intelligent Robots and Systems (IROS '10)*, pp. 5919–5926, Taipei, Taiwan, October 2010.
- [106] M. Saha and P. Isto, "Motion planning for robotic manipulation of deformable linear objects," in *Proceedings of the IEEE International Conference on Robotics and Automation (ICRA '06)*, pp. 2478–2484, Orlando, Fla, USA, May 2006.
- [107] A. Kapadia, E. Tatlicioglu, and I. D. Walker, "Teleoperation control of a redundant continuum manipulator using a non-redundant rigid-link master," in *Proceedings of the IEEE/RSJ International Conference on Intelligent Robots and Systems (IROS '12)*, pp. 3105–3110, Vilamoura, Portugal, 2012.
- [108] M. Csencsits, B. A. Jones, W. McMahan, V. Iyengar, and I. D. Walker, "User interfaces for continuum robot arms," in *Proceedings of the IEEE IRS/RSJ International Conference on Intelligent Robots and Systems, IROS 2005*, pp. 3011–3018, Edmonton, Canada, August 2005.
- [109] W. McMahan and I. D. Walker, "Octopus-inspired grasp synergies for continuum manipulators," in *Proceedings of the IEEE International Conference on Robotics and Biomimetics*, pp. 945–950, Bangkok, Thailand, 2009.
- [110] Y. Yekutieli, R. Sagiv-Zohar, B. Hochner, and T. Flash, "Dynamic model of the octopus arm. II: control of reaching movements," *Journal of Neurophysiology*, vol. 94, no. 2, pp. 1459–1468, 2005.
- [111] A. Kapadia and I. D. Walker, "Self-Motion analysis of extensible continuum manipulators," in *Proceedings of the IEEE International Conference on Robotics and Automation*, Karlsruhe, Germany, May 2013.
- [112] I. S. Godage, T. Nanayakkara, and D. G. Caldwell, "Locomotion with continuum limbs," in *Proceedings IEEE/RSJ International Conference on Intelligent Robot Systems (IROS '12)*, pp. 293–298, Vilamoura, Portugal, 2012.
- [113] I. D. Walker, "Continuum robot appendages for traversal of uneven terrain in in situ exploration," in *Proceedings of the IEEE Aerospace Conference (AERO '11)*, Big Sky, Mont, USA, March 2011.
- [114] M. Sfakiotakis, A. Kazakidi, N. Pateromichelakis, J. A. Eka-terinaris, and D. P. Tsakiris, "Robotic underwater propulsion inspired by the octopus multi-arm swimming," in *Proceedings of the IEEE International Conference on Robotics and Automation*, pp. 3833–3839, St. Paul, Minn, USA, 2012.
- [115] L. Cowan and I. D. Walker, "The importance of continuous and discrete elements in continuum robots," *International Journal of Advanced Robot Systems*, vol. 10, pp. 1–13, 2013.
- [116] A. Kapoor, N. Simaan, and R. H. Taylor, "Suturing in confined spaces: constrained motion control of a hybrid 8-DoF robot," in *Proceedings of the 12th International Conference on Advanced Robotics (ICAR '05)*, pp. 452–459, Seattle, Wash, USA, July 2005.
- [117] A. Kapoor, K. Xu, W. Wei, N. Simaan, and R. H. Taylor, "Telemanipulation of snake-like robots for minimally invasive surgery of the upper airway," in *Proceedings of the 9th International Conference on Medical Image Computing and Computer-Assisted Intervention (MICCAI) Medical Robotics Workshop*, 2006.
- [118] G. P. Scott, C. G. Henshaw, D. Walker, and B. Willimon, "Autonomous robotic refueling of an unmanned surface vehicle in varying sea states," submitted to *Journal of Field Robotics*.
- [119] J. Merino, A. L. Threath, I. D. Walker, and K. E. Green, "Kinematic models for continuum robotic surfaces," in *Proceedings of the IEEE/RSJ International Conference on Intelligent Robots and Systems (IROS '12)*, pp. 3453–3460, Vilamoura, Portugal, 2012.



Hindawi

Submit your manuscripts at
<http://www.hindawi.com>

